

ARTICLES

Photoelectrochemical Properties of Poly(3,4-ethylenedioxythiophene)

E. M. Giroto, W. A. Gazotti, and M.-A. De Paoli*

*Laboratório de Polímeros Condutores e Reciclagem, Instituto de Química,
Universidade Estadual de Campinas, C.P. 6154, 13083–970 Campinas, SP, Brazil**Received: December 20, 1999; In Final Form: March 10, 2000*

The photoelectrochemical properties of poly(3,4-ethylene dioxythiophene)/poly(styrene sulfonate) in contact with an electrolytic solution containing a redox couple were studied using the theories for the semiconductor–electrolyte interface. When this polymer–electrolyte interface is illuminated with $h\nu > E_g$ (gap energy) it exhibits cathodic photocurrent typical of *p*-type semiconductors, and the flat band potential, density of majority carriers, and the depletion layer thickness can be determined. To complete the band energy diagram of this polymer–electrolyte interface we obtained the band gap energy through the absorption and photocurrent spectra. The relatively low band gap energy (1.5 eV) and the photoeffects observed at the interface suggest its use as the absorbing material in photoelectrochemical cells.

Introduction

Basic properties of semiconductors and the phenomena which occur at the semiconductor–electrolyte interface in the dark have been discussed in the literature.^{1,2} Based on these theories we can study the characteristics of these interfaces illuminated with mono- or polychromatic radiation. A considerable part of the most recent studies involving the use of organic materials in electrooptical technology concerns polymeric semiconductors.^{3,4} Their properties are similar to those found for inorganic semiconductors, suggesting their use in photoelectrochemical cells. The science and technology of such devices has developed during the last years as the result of the increasing demand, low cost, and environmental impact of energy production. Thus knowledge of organic semiconductor interfaces is important to permit the design of new photoelectrochemical cells.

When a semiconductor modified electrode is in contact with an electrolytic solution, a charge transfer occurs through the interface providing equilibrium between the Fermi level of the semiconductor and the redox potential of the solution.⁵ Irradiating the semiconductor with $h\nu > E_g$, valence band electrons are promoted to the conduction band. Thus, mobile states of electron–hole pairs (excitons) are created. For amorphous semiconductors, Coulombic interactions between the carriers cannot be neglected and recombination becomes significant. In *p*-type semiconductors minority carriers (electrons) migrate toward the interface, while majority carriers (holes) diffuse to the semiconductor bulk. At the boundary, oxidized species in the electrolytic solution are reduced by the electrons, being regenerated at the counterelectrode and resulting in photocurrent in a short-circuited system. For *n*-type semiconductors the majority carriers are the electrons and an inverse behavior occurs.

Interfacial electrochemistry theories are useful tools to study the polymer–electrolyte interface here described. A common

aspect in all electrode–electrolyte interfaces is the formation of electrically charged layers (ionic charge in the electrolyte and electronic in the electrode) with a capacitance related to these interfaces. For semiconductor electrodes a special situation occurs: these materials have low density of charge carriers in comparison to metals. Thus, the electrically charged layer at the semiconductor (space charge region) is larger than that formed in the electrolyte. This situation induces the formation of an electric field in the space charge region, leveling the semiconductor Fermi level and the redox potential of the electrolytic solution and producing a band bending close to the electrolyte boundary. This electric field is responsible for electron and hole transport at the interface, when they are in excess. At the surface, the semiconductor becomes depleted of majority carriers and a depletion layer, *W*, is formed. The potential where no excess of charge exists is called “zero charge potential.” In this condition we do not have an electric field, the space charge region disappears, and the bands do not bend. The potential where this situation occurs is known as “flat band potential,” E_{FB} .

We have previously studied the photoelectrochemical properties of some polymeric semiconductors: polypyrrole,^{6,7} polyaniline,^{6,8,9} poly(*o*-methoxyaniline),¹⁰ and poly(3-methylthiophene).^{6,11} Poly(3,4-ethylene dioxythiophene) is another example of this class of materials and has been studied due to its high conductivity in the oxidized form and low band gap energy in comparison to other polythiophenes.^{12,13} In a recent paper we used poly(3,4-ethylene dioxythiophene)/poly(styrene sulfonate) (PEDT-PSS) to assemble an all-plastic electrochromic device, based on its optical properties.¹⁴ In the present work we investigate its photoelectrochemical properties aiming to assemble photovoltaic devices or photosensors.

Experimental Section

Thin films of poly(3,4-ethylene dioxythiophene)/poly(styrene sulfonate) were obtained by casting from its commercial solution

* Corresponding author. E-mail: mdepaoli@iqm.unicamp.br.

Baytron-P (Bayer A. G., Germany) on plastic conductive substrates (ITO-PET, I. S.T, sheet resistance of $60 \Omega/\text{square}$, area = 1.0 cm^2). The thickness of the films was $0.7 \mu\text{m}$, measured with a Tencor Instruments Alpha-Step 200. The ITO electrodes were previously cleaned with distilled water, and then ethanol, and dried under atmospheric conditions. The electrolyte was a $0.1 \text{ M } (\text{C}_4\text{H}_9)_4\text{NBF}_4$ (Aldrich, used as received) solution in dry distilled acetonitrile. The effect of different redox couples was evaluated by using nondegassed or degassed electrolyte solutions or by adding the iodine/triiodide redox couple. In this last case, I_2/I^- concentrations were 1 and 10 mM , respectively. A Pt wire was used as counterelectrode and Ag—AgCl as the reference electrode in a one compartment cell. The cell was fixed on an optical bench and connected to a PGSTAT10 AutoLab potentiostat. The electrode was illuminated with a 200 W Xe (Hg) lamp regulated by an Oriel power supply (Model 66001) and a Jarrel-Ash (Model 82410) monochromator. A lock-in amplifier (EG&G PAR, Model 521) and a variable frequency chopper (EG&G PAR, Model 192) were also used. All irradiations were carried out using a water filter (Oriel, Model 6214) to minimize thermal effects. Photocurrent spectra were obtained by normalizing the incident monochromatic light in relation to the response of a calibrated silicon photodetector (Newport, Model 818-UV) controlled by an optical power meter (Newport, Model 1830-C). No corrections were made for reflection or absorption of the electrodes. All experiments were done under atmospheric conditions, at 22°C and relative ambient humidity between 40 and 60%. Polychromatic light intensity at the samples was 95 mWcm^{-2} and the electrochemical cell was always irradiated from the polymer—electrolyte interface side (EE).

Results and Discussion

A very common and sensitive technique to measure the photocurrent at an electrode—electrolyte interface resides in illuminating the system with modulated light and detecting the current through a lock-in amplifier. The frequency of the chopped polychromatic light was chosen by submitting the polymer films to -0.2 V (vs. Ag—AgCl, electrolyte: $0.1 \text{ mol L}^{-1} (\text{C}_4\text{H}_9)_4\text{NBF}_4$ containing I_2/I^-) and measuring the modulated photocurrent as a function of the frequency of the chopper. The photoeffects observed are strongly dependent on the irradiation frequency and a maximum was observed at 10 Hz , corresponding to a response time of 100 ms , longer than those observed for inorganic semiconductors. The long response time is probably due to slow structural rearrangements of polymer chains and counteranion diffusion that occurs during the photoprocesses, however, the response time obtained for PEDT-PSS is short when compared to other conducting polymers, like poly(3-methyl-thiophene).¹⁵

Figure 1 shows the photocurrent registered by a lock-in amplifier during cyclic voltammograms of PEDT-PSS films under modulated polychromatic illumination (95 mW cm^{-2} , 10 Hz). Experiments performed using an argon purged solution (Figure 1a) do not show photocurrent because a redox couple is necessary to complete the charge transport in a photoelectrochemical cell. Photoeffects are observed by adding NaI/I_2 to the Argon purged electrolyte (Figure 1b) and using a nonpurged electrolyte solution, where oxygen also plays the role of the redox pair, O_2/O_2^- (Figure 1c). Figure 1b shows that iodine/triiodide is a reasonable redox couple to detect photoeffects in this system; however, higher photocurrent is obtained using an oxygen saturated electrolyte. Several authors have described the photoelectrochemical reduction of dissolved oxygen in solutions

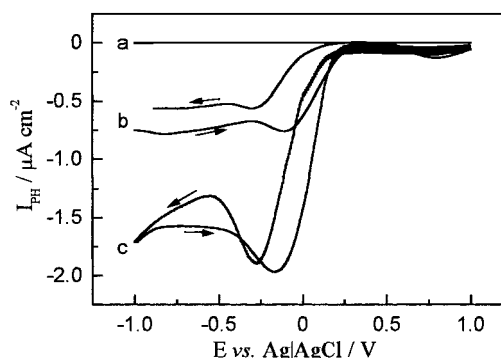


Figure 1. Photocurrent density registered during a cyclic voltammetry (10 mV s^{-1}) of PEDT-PSS films in different $0.1 \text{ mol L}^{-1} (\text{C}_4\text{H}_9)_4\text{NBF}_4$ acetonitrile solutions: (a) purged with argon, (b) purged with argon and containing I_3^-/I^- , (c) oxygen saturated.

that do not contain another redox couple.^{16–17} According to Garnier et al.,¹⁸ electrons generated in the photoelectrochemical process reduce dissolved O_2 . In the present system the participation of O_2 as the redox species was confirmed by an abrupt decrease of the photoresponse when purging the solution with argon and restoration of the photoresponse after the interruption of the argon flux. The initial value is achieved when the solution is again saturated with oxygen, indicating that this process is reversible.

Photocurrent signals registered in the potential scans shown in Figure 1 also indicate that PEDT-PSS is photoactive only in its reduced form, independently on the redox couple in the electrolyte solution. At anodic potentials, the polymer is oxidized and has high electric conductivity ($\sim 200 \text{ S cm}^{-1}$).¹² The high conductivity favors the recombination processes and no photocurrent is observed. Hysteresis observed in these curves are typical for this class of materials and are related to conformational changes occurring during the redox processes. The cathodic signal of the photocurrent shows that PEDT-PSS has a *p*-type semiconductor behavior.

The maximum of photocurrent in Figure 1 ($-2.0 \mu\text{Acm}^{-2}$) occurs at -0.17 V with the oxygen saturated electrolyte and -0.11 V ($-0.8 \mu\text{Acm}^{-2}$) using iodine/triiodide as the redox couple, respectively. Lower photocurrent values observed in the last case are probably due to absorption of part of the incident visible light by I_3^-/I^- . The photoresponse is more intense when using the nonpurged electrolyte and all results described below were obtained using O_2 as redox species.

The flat band potential, E_{FB} , is an important parameter to characterize a semiconductor electrode and, for a *p*-type semiconductor, is the upper limit of a blocking potential region where the electrode response is dominated by the “space charge region” behavior. We used two methods to calculate E_{FB} .

According to Butler,¹⁹ if the energy of the incident light is tuned to a value close to E_g , where the absorption coefficient is small, the current under illumination becomes proportional to the space charge region thickness. Equation 1²⁰ takes into account these assumptions, where ϵ_0 is vacuum permittivity, ϵ is the dielectric constant of the semiconductor, e is the electronic charge, I_0 is the incident light intensity, α is the absorption coefficient, and N is the density of carriers. A plot of the square of the photocurrent versus potential yields a straight line and its interception with the *x*-axis corresponds to E_{FB} . Figure 2 shows the plot of I_{PH}^2 versus E , from which we obtained $E_{\text{FB}} = 0.20 \text{ V}$. Photocurrent values were obtained by polarizing the polymer modified electrode at different potentials in chronoamperometric experiments, illuminating the electrode with chopped light (10 Hz) and measuring photocurrent signals with

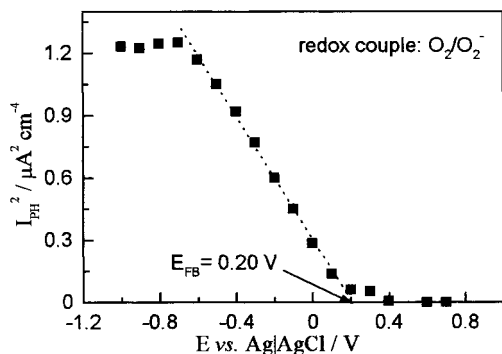


Figure 2. Variation of the square of photocurrent density as a function of applied potential, obtained from chrono-amperometric experiments using a lock-in amplifier and a chopped light beam at 10 Hz.

a lock-in amplifier.

$$I_{\text{PH}}^2 = 2e \left(\frac{\epsilon \epsilon_0 \alpha^2 I_0}{N} \right) (E - E_{\text{FB}}) \quad (1)$$

Another way to estimate E_{FB} is measuring the differential capacitance of the semiconductor–electrolyte interface. This parameter can be represented by several capacitances in series, eq 2,²¹ where C_{SC} is the space charge layer capacitance, C_{H} is the Helmholtz double layer capacitance, C_{G} the Gouy–Chapman layer capacitance, and C_{SS} is the surface state capacitance.

$$\frac{1}{C} = \frac{1}{C_{\text{H}}} + \frac{1}{C_{\text{G}}} + \frac{1}{C_{\text{SC}} + C_{\text{SS}}} \quad (2)$$

In a series of capacitors, the smallest one determines the overall capacitance. In concentrated electrolytes, C_{G} is large and can be neglected. Helmholtz capacitance is generally several orders of magnitude greater than C_{SC} and can also be neglected. Thus, if the surface states density is low, the total capacitance can be estimated by the space charge capacitance, C_{SC} . In the depletion layer condition, C_{SC} obeys the Mott–Schottky relation, eq 3,² where T is the absolute temperature and k is the Boltzmann constant. Thus, the value of E_{FB} is obtained from the intercept with the potential axis of the linear part of the plot of C_{SC}^{-2} versus potential.

$$C_{\text{SC}}^{-2} = \left(\frac{2}{\epsilon \epsilon_0 e N A^2} \right) \left(E - E_{\text{FB}} - \frac{kT}{e} \right) \quad (3)$$

Capacitance values used to construct the Mott–Schottky plots were estimated from the capacity current (I_{c}) obtained in AC voltammetry measurements in the dark and under illumination with polychromatic radiation of 95 mW cm⁻². In these experiments a sinusoidal signal with an amplitude (V_{rms}) of 0.01 V and frequency of 250 Hz was applied to the working electrode during a voltammetry measurement. I_{c} values were used in eq 4 to calculate C .

$$C = \frac{I_{\text{c}}}{2\pi f V_{\text{rms}}} \quad (4)$$

Figure 3 shows the Mott–Schottky plots for the system in the dark and under illumination. From these plots we obtained $E_{\text{FB}} \approx 0.21$ V, which is very close to the value obtained from the plot in Figure 2. The agreement between the E_{FB} values obtained by the two methods indicates the validity of neglecting C_{H} , C_{G} , and C_{SS} for this system.

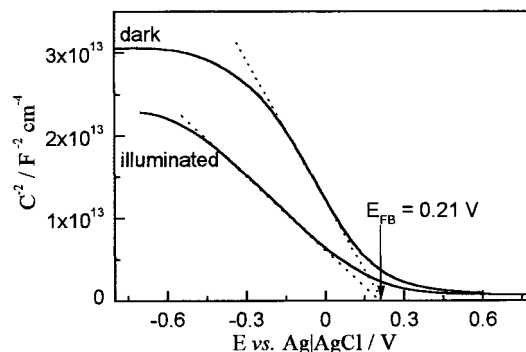


Figure 3. Mott–Schottky plots for PEDT-PSS films obtained from AC voltammetry measurements in the dark and under illumination.

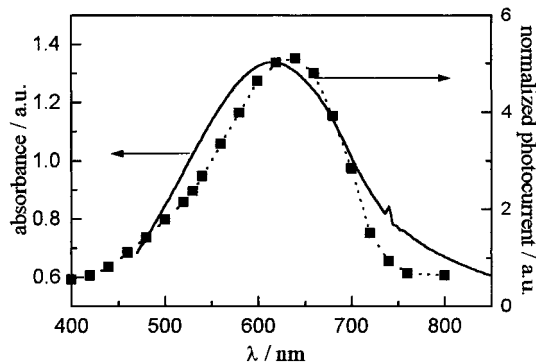


Figure 4. Comparison of the (—) absorbance and (■) photocurrent spectra (under EE irradiation) for a reduced PEDT-PSS film.

Mott–Schottky plots can also be useful to estimate the density of charge carriers. Considering $\epsilon = 10$, according to the literature,²¹ the densities of charge carriers for PEDT-PSS were calculated; $N_{\text{D}} = 2.6 \times 10^{17}$ cm⁻³ in the dark and $N_{\text{L}} = 5.2 \times 10^{17}$ cm⁻³ under illumination. Both results are comparable to those obtained for inorganic semiconductors²⁰ or conducting polymers,²² but possible deviations from real values are expected because this model does not take into account the roughness and porosity of the conducting polymer modified electrode, nor the dependence of its dielectric constant on its oxidation state. However, these deviations equally influences the values of N in the dark or under illumination and the variation observed when the cell is illuminated ($N_{\text{L}} = 2N_{\text{D}}$) evidences the photoelectrochemical effect.

N values can be used to evaluate the depletion layer width (W), as shown in eq 5,²³ where E is the potential when $C_{\text{SC}}^{-2} = 0$ in the Mott–Schottky plot. We calculated $W = 100$ Å in the dark and $W = 70$ Å under illumination. The decrease of W under illumination is an expected situation due to the injection of carriers into the depletion layer. The same trend is observed when the photoconductivity phenomenon is observed.²⁴

$$W = \sqrt{\frac{2\epsilon \epsilon_0 E}{eN}} \quad (5)$$

The energy gap of a semiconductor can be estimated by its absorption edge. The absorption spectrum of the polymer film in the reduced state shows a broad absorption in the 500 to 700 nm range, Figure 4; this is caused by the different π -electron conjugation length of the polymer chains. From this spectrum we estimate the optical band gap edge in the range of 1.6 (775 nm) to 1.5 eV (840 nm) and an absorption maximum at 2.0 eV (620 nm), which are similar to those described in the literature.¹² The reasonable agreement between the absorbance and the photocurrent spectra obtained with the photoelectrochemical cell

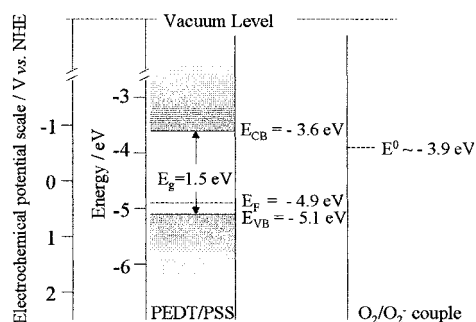


Figure 5. Energy diagram of PEDT-PSS in contact with a 0.1 M $(\text{C}_4\text{H}_9)\text{NBF}_4$ acetonitrile solution, at 22 °C.

irradiated from the EE interface, Figure 4, indicates that the Schottky barrier occurs at the polymer–electrolyte interface.

As mentioned above, when the polymer is immersed into the electrolyte solution, an equilibrium occurs involving changes in the semiconductor Fermi level and the redox potential of the solution. In the flat band potential there is no charge transfer and we can assume that in this situation $E_{\text{FB}} = E_{\text{F}}$.²⁵ Taking into account these considerations, we constructed the band energy diagram, converting the values to an energy scale using $E \text{ (eV)} = -4.5 - E \text{ (V)}$, where the electrochemical potential is related to the normal hydrogen electrode (NHE). When the PEDT-PSS film is in contact with the electrolyte and O_2 is the electron acceptor, $E_{\text{FB}} = 0.2 \text{ V}$ (vs. $\text{Ag}–\text{AgCl}$) or $\sim 0.4 \text{ V}$ (vs. NHE) and for the redox couple, $E^0 \sim -0.6 \text{ V}$ (vs. NHE). Recalculating these values, we have $E_{\text{FB}} = -4.9 \text{ eV}$ and $E^0 \sim -3.9 \text{ eV}$. For this we assumed $E_{\text{g}} = 1.5 \text{ eV}$. Considering the difference between the Fermi level and the top of the valence band is 0.2 eV ,²³ the energy diagram for PEDT-PSS can be sketched, Figure 5. Such an energy diagram can roughly explain why this polymer forms a rectifying contact with the O_2/O_2^- couple and an ohmic contact with ITO (work function $\sim 4.7 \text{ eV}$).²⁶

Conclusions

When reduced PEDT-PSS films are in contact with an electrolyte containing a redox couple and are illuminated with $h\nu > E_{\text{g}}$, a cathodic photocurrent is observed, typical of *p*-type semiconductors. The response time for the occurrence of the photoeffects is 100 ms, which is shorter than those observed for other polythiophenes in the same conditions.¹¹

Based on classical semiconductor theories we evaluated the flat band potential of this polymer and the results allow the estimation of the density of charge carriers and the depletion layer thickness. The estimated density of charge carriers is in agreement with the values found for inorganic semiconductors and conducting polymers, although we neglected some factors, such as the roughness and porosity of polymer films and changes

in the dielectric constant of the material as a function of its oxidation state. The increase of the density of charge carriers when the film is illuminated evidences the photogeneration of charge carriers.

The energy diagram for the interface was calculated and used to explain why PEDT-PSS forms a Schottky barrier with the electrolyte and an ohmic contact with ITO electrodes. Finally, this conducting polymer exhibits a low band gap energy (1.5 eV) and short response time ($\sim 100 \text{ ms}$) when compared to other conducting polymers, indicating that it can be used in photoelectrochemical cells as an absorbing material.

Acknowledgment. The authors thank FAPESP for fellowships (Processes number 97/02156-3 and 97/14132-1) and financial support (Process number 96/09983-0) and Bayer (Brazil) for the donation of Baytron-P.

References and Notes

- (1) Koryta, J.; Dvorak, J.; Kavan, L. *Principles of Electrochemistry*, 2nd ed.; John Wiley: New York, 1993.
- (2) Bard, A. J.; Faulkner, L. R. *Electrochemical Methods—Fundamentals and Applications*; John Wiley: New York, 1980.
- (3) Bantikasagn, W.; Inganäs, O. *Thin Solid Films* **1995**, 293, 138.
- (4) Camaioni, N.; Casalbore-Miceli, G.; Geri, A.; Zotti, G. *J. Phys. D: Appl. Phys.* **1998**, 31, 1245.
- (5) Gerischer, H. *Electrochim. Acta* **1990**, 35, 1677.
- (6) Miquelino, F. L. C.; De Paoli, M.-A.; Geniès, E. M. *Synth. Met.* **1994**, 68, 91.
- (7) Martini, M.; De Paoli, M.-A. *Sol. Energy Mater. Sol. Cells* **2000**, 60, 73.
- (8) das Neves, S.; De Paoli, M.-A. *Synth. Met.* **1998**, 96, 48.
- (9) Maia, D. J.; das Neves, S.; Alves, O. L.; De Paoli, M.-A. *Electrochim. Acta* **1999**, 44, 1945.
- (10) Gazotti, W. A.; Faez, R.; De Paoli, M.-A. *J. Electroanal. Chem.* **1996**, 415, 107.
- (11) Micaroni, L.; De Paoli, M.-A. *Sol. Energy Mater. Sol. Cells* **1996**, 46, 79.
- (12) Pei, Q.; Zucarello, G.; Ahlskog, M.; Inganäs, O. *Polymer* **1994**, 35, 1347.
- (13) Dietrich, M.; Heinze, J.; Heywang, G.; Jonas, F. *J. Electroanal. Chem.* **1994**, 369, 87.
- (14) De Paoli, M.-A.; Casalbore-Miceli, G.; Gazotti, W. A.; Giroto, E. M. *Electrochim. Acta* **1999**, 44, 2983.
- (15) Micaroni, L.; Polo da Fonseca, C. N.; Decker, F.; De Paoli, M.-A. *Sol. Energy Mater. Sol. Cells* **2000**, 60, 127.
- (16) Abrantes, L. M.; Castillo, L. M.; Fleischmann, M.; Hill, I. R.; Peter, L. M.; Mengoli, G.; Zotti, G. *J. Electroanal. Chem.* **1984**, 177, 129.
- (17) Li, Z.; Dong, S. *Electrochim. Acta* **1992**, 37, 1003.
- (18) Glenis, S.; Tourillon, G.; Garnier, F. *Thin Solid Films* **1986**, 139, 221.
- (19) Butler, M. A. *J. Appl. Phys.* **1977**, 48, 1914.
- (20) Finklea, H. *Semiconductors Electrodes*; Elsevier: New York, 1988.
- (21) Sunde, S.; Hagen, G.; Odegard, R.; *J. Electroanal. Chem.* **1993**, 345, 59.
- (22) Glenis, S.; Tourillon, G.; Garnier, F. *Thin Solid Films* **1984**, 122, 9.
- (23) Wilson, R. H. *J. Appl. Phys.* **1977**, 48, 4292.
- (24) Skotheim, T. *Appl. Phys. Lett.* **1981**, 38, 9.
- (25) Gerischer, H. In *Photovoltaic and Photoelectrochemical Solar Energy Conversion*; Cordon, S.; Gomes, W. P.; Dekeyser, W., Eds.; Plenum Press: New York, 1981.
- (26) Wöhrle, D.; Meissner, D. *Adv. Mater.* **1991**, 3, 129.